

## Towards an Experimental Protocol for the Study of Induction Heating in Asphalt Mastics

Apostolidis, Panos; Liu, X.; Scarpas, Athanasios; van Bochove, G; van de Ven, Martin

**Publication date**

2016

**Document Version**

Accepted author manuscript

**Published in**

Transportation Research Board 95th annual meeting

**Citation (APA)**

Apostolidis, P., Liu, X., Scarpas, A., van Bochove, G., & van de Ven, M. (2016). Towards an Experimental Protocol for the Study of Induction Heating in Asphalt Mastics. In *Transportation Research Board 95th annual meeting*

**Important note**

To cite this publication, please use the final published version (if applicable).  
Please check the document version above.

**Copyright**

Other than for strictly personal use, it is not permitted to download, forward or distribute the text or part of it, without the consent of the author(s) and/or copyright holder(s), unless the work is under an open content license such as Creative Commons.

**Takedown policy**

Please contact us and provide details if you believe this document breaches copyrights.  
We will remove access to the work immediately and investigate your claim.

# Towards an Experimental Protocol for the Study of Induction Heating in Asphalt Mastics

P. Apostolidis<sup>1</sup>, X. Liu<sup>1</sup>, T. Scarpas<sup>1</sup>, G. van Bochove<sup>2</sup> and M.F.C. van de Ven<sup>1</sup>

<sup>1</sup> Section of Pavement Engineering

Faculty of Civil Engineering and Geosciences, Delft University of Technology

Stevinweg 1, 2628 CN Delft, the Netherlands

Tel. +31 61 6599128, Email: [p.apostolidis@tudelft.nl](mailto:p.apostolidis@tudelft.nl)

<sup>2</sup> Heijmans, Heijmans Integrale Projecten B.V.

Graafsebaan 3, 5248 JR Rosmalen, the Netherlands

Tel. +31 73 5435425, Email: [gbochove@heijmans.nl](mailto:gbochove@heijmans.nl)

Corresponding author:

P. Apostolidis

E-mail: [p.apostolidis@tudelft.nl](mailto:p.apostolidis@tudelft.nl)

Total Number of Words

Words in abstract	=	186	words
Words in text:	=	4199	words
Words in references	=	582	words
Tables: (1x250)	=	250	words equivalent
Figures: (9x250)	=	2250	words equivalent
Total	=	7467	words equivalent

*Submitted for publication and presentation for the 95<sup>th</sup> meeting of the Transportation Research Board, January 10-14, 2016*

# **Towards an Experimental Protocol for the Study of Induction Heating in Asphalt Mastics**

P. Apostolidis<sup>1</sup>, X. Liu<sup>1</sup>, T. Scarpas<sup>1</sup>, G. van Bochove<sup>2</sup> and M.F.C. van de Ven<sup>1</sup>

## **ABSTRACT**

The development of asphalt mixtures with improved electrical and thermal properties is crucial in terms of producing suitable mixtures for the induction heating without losing their durability. The main scope of this research is to evaluate experimentally the impact of filler-sized electrically conductive additives on the induction heating efficiency and the rheological performance of asphalt mixtures. Within this framework, an experimental assessment protocol of structural and non-structural important parameters of induction heated asphalt mastics – asphalt mixtures without stone aggregates and sand – was developed. It was observed that by adding iron powder as filler-sized conductive additive to asphalt mastics the electrical and thermal properties improve. Moreover, the rheological investigations of different conductive asphalt mastics show the importance of adding iron powder after replacing the amount of mineral filler in order to maintain the workability of mastics. The micro-morphological observation of asphalt mastics using scanning electron microscopy illustrates the impact of filler-size particles – minerals and conductive additives – on the skeleton of asphalt mastics.

## 1 INTRODUCTION

2  
3 Today, the rapid growth of the transportation infrastructure around the world and the need to focus more on  
4 environmental friendly solutions for the construction and maintenance of pavements is leading the asphalt  
5 paving industry to explore novel technological improvements. With the impending European and global  
6 regulations on greenhouse gas emissions, fumes and energy conservation, these demands are becoming  
7 increasingly challenging (1-3). Meanwhile a lot of effort is on developing sustainable asphalt mixtures with  
8 non-structural properties by integrating new functionalities without losing their durability. One of these non-  
9 structural functionalities is induction heating. Induction heating asphalt mixtures have attracted considerable  
10 attention as conductive mixtures capable to restore their mechanical properties under induction energy (4-10).

11 With regard asphalt pavement maintenance, there are various techniques that can be used to restore the  
12 mechanical characteristics of mixtures during their lifespan. The induction heating is one of these and a  
13 promising technique to prolong the service life of asphalt pavements by speeding up the self-healing process  
14 of asphalt. In order to increase the efficiency of induction heating, new mixtures with electrically conductive  
15 additives need to be developed. The contribution of these additives is to create asphalt mixtures with  
16 improved electrical and thermal properties, suitable for induction heating.

17 To study the new asphalt mixtures for induction heating, it is important to have in-depth understanding of  
18 the interaction between the conductive additives and other asphalt components. Because of the fact that the  
19 improved macroscopic response of an asphalt pavement has a direct link with the durability of the bonding  
20 components in the asphalt mixtures, much research is focused on the behavior of asphalt mastics (binder and  
21 filler-sized particles) and mortars (binder, filler-sized particles and sand). Particularly, the influence of filler-  
22 to-binder interaction on mastic performance (11-12) and the volumetric concentration of different types of  
23 fillers (13) are studied at mastic level. On the other hand, asphalt mortars have been studied extensively in  
24 (14-15).

25 To develop conductive asphalt mixtures suitable for induction heating, many efforts were concentrated on  
26 adding fiber-type conductive particles (e.g. steel fibers or steel wool) in order to improve the durability of  
27 mixtures and increase the induction heating efficiency. However, mixtures with steel fibers require a strong  
28 mixing effort and longer mixing time to disperse steel fibers uniformly. Especially, the longer steel fibers  
29 easily produce clusters inside the asphalt mixtures, causing inhomogeneity and reducing the mechanical  
30 response (9, 10). Apart from the performance degradation because of the large amounts of fiber-type  
31 additives, this type of additives can result significant increase of cost (17). For this reason and in order to  
32 resolve the problems resulted by the fiber-type particles, conductive asphalt mixtures can be produced by  
33 adding filler-sized conductive particles.

34 The effective properties of asphalt mixtures vary considerably according to the type and the characteristics  
35 of filler-sized conductive additives. Higher conductivity of additives results in higher conductivity of the  
36 asphalt concrete (18). Moreover, the volumetric concentration of particles affects on the effective  
37 conductivity of asphalt mixture. Carbon black (18) and graphite powder (4, 18, 19) are among the examples  
38 of filler-sized particles that were used to improve electrical conductivity of asphalt mixture. Also it is known  
39 from previous researches that carbon black and graphite powder appear to have excellent compatibility with  
40 asphalt binder imparting in parallel easy mixing. However, no extended research has focused on other types  
41 of filler-sized conductive additives and subsequently on additives for developing asphalt concrete mixtures  
42 for induction heating application.

43 In this paper, iron powder is selected as filler-sized additive with very high electrical conductivity and its  
44 interaction with the conventional components of asphalt mastic is studied. For a certain asphalt binder,  
45 asphalt mastics with different volumetric properties are developed and characterized following a new  
46 experimental protocol designed for this purpose. Initially, the evaluation of physical properties of mineral  
47 fillers and iron powder is required before the development of conductive asphalt mastics. To study in detail

48 the micro-morphology of different conductive asphalt mastics scanning electron microscopy (SEM) is  
 49 utilized. As mentioned above, the performance of asphalt mastic is associated with the skeleton of filler  
 50 particles inside and for this reason the micro-morphology of mastic surface is examined. Furthermore,  
 51 electrical, thermal and rheological properties of conductive asphalt mastics are determined by using a digital  
 52 multimeter, a thermal sensor and dynamic shear rheometer (DSR), respectively. The finding of the current  
 53 research will contribute to understand the influence of filler-sized conductive additives on the mechanical  
 54 performance of asphalt mastics designed for induction heating applications.

## 55 **INDUCTION HEATING APPROACH OF CONDUCTIVE ASPHALT MIXTURES**

56  
 57  
 58 Induction heating is adapted as a maintenance technique for asphalt pavements and requires the development  
 59 of conductive asphalt mixtures. For this reason, conductive additives are mixed within the mixtures and an  
 60 alternating magnetic field is applied. This field induces eddy currents in the additives and consequently heats  
 61 them according to the principles of Joule's law, see Figure 1.c. The generated heat in the additives increases  
 62 the temperature of the asphalt mixture around them, through the temperature rise the bitumen is melting, the  
 63 micro-cracks are healed and the pavement is treated. In particular, induction power heats locally the mastic  
 64 part of asphalt concrete and because of diffusion and flow of bitumen the cracks are healed without damaging  
 65 the stone skeleton. According to Faraday's law, the electromotive force from the magnetic field is:

$$66 \quad \varepsilon = - \frac{d\phi B}{dt} \quad (1)$$

67  
 68 where  $\varepsilon$  is the electromotive force,  $\frac{d\phi}{dt}$  is the momentary angular velocity and B is the magnetic flux.

69 Based on Joule's first law, the alternating electric currents generate heat in the additives. Consequently,  
 70 power dissipation occurs locally on the mixture and it is expressed in terms of exposure time t as:

$$71 \quad Q = I^2 R t \quad (2)$$

72  
 73 where I is the amount of current and R is the effective electrical resistance of the conductive mixture with  
 74 additives.

75 The alternating electric current through the conductive mixture with effective resistance R is:

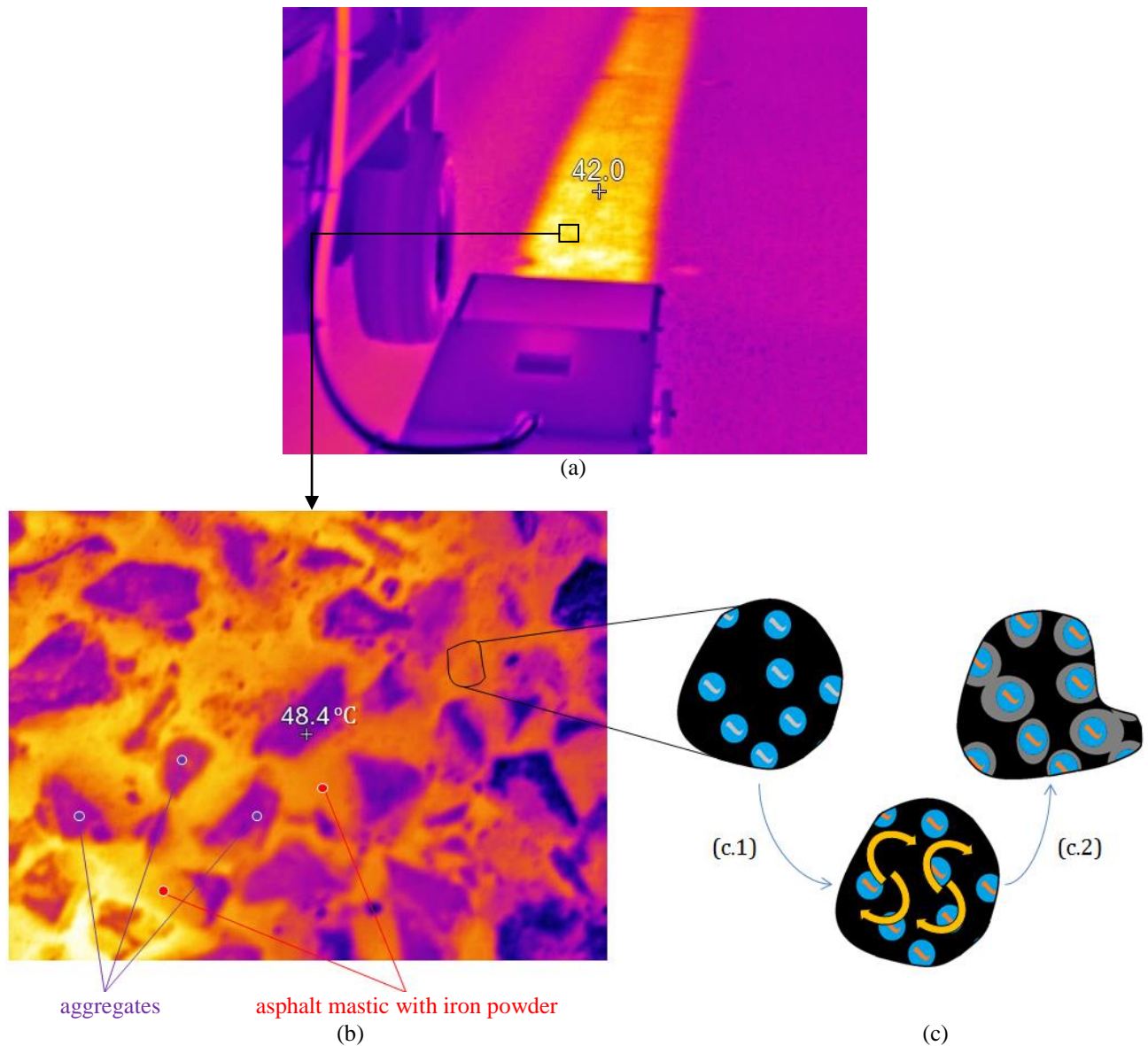
$$76 \quad I = \frac{\varepsilon}{R} \quad (3)$$

77  
 78 and by substituting the above equation for the current into one or both factors of current in Joule's law, the  
 79 power dissipated on the asphalt mixture can be rewritten in the equivalent form:

$$80 \quad Q = \frac{\varepsilon^2}{R} \cdot t \quad (4)$$

81  
 82 The induction heating efficiency depends on the operational parameters, such as frequency, power, and the  
 83 effective properties of asphalt mixtures. In this paper, as previously mentioned, the induction heating  
 84 efficiency is investigated of additives on the asphalt mastics under constant operational conditions.

85



86  
 87 **FIGURE 1** Infrared image (a) during induction heating of an asphalt pavement (A58 near Vlissingen,  
 88 the Netherlands), (b) of heated asphalt pavement surface at high resolution and (c) the schematic of  
 89 induction heating of an asphalt mixture (c.1) induced by eddy currents and (c.2) heat generation in the  
 90 mixture based on the Joule's law

91

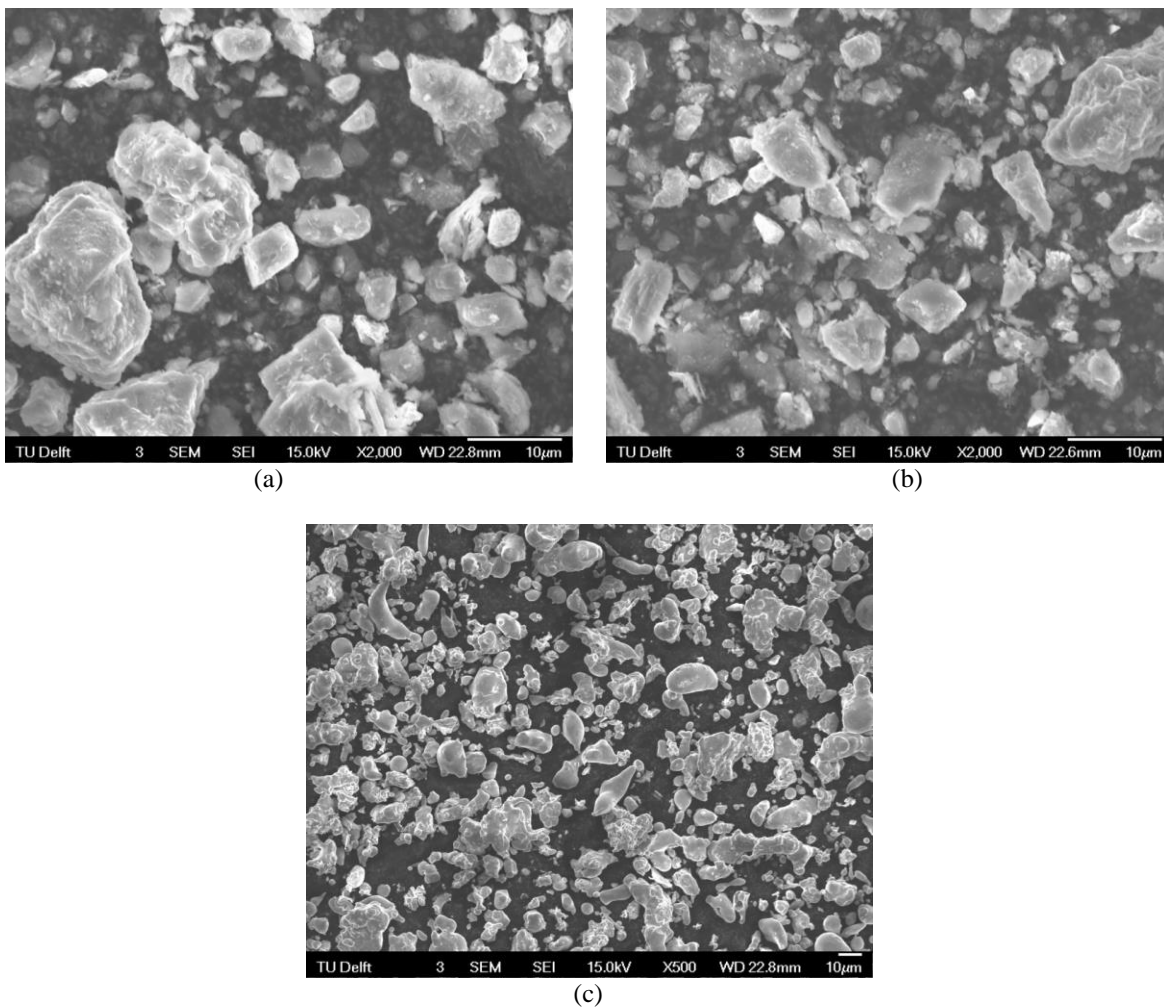
## 92 MATERIAL AND PREPARATION

93

94 Firstly, the selected fillers and filler-sized conductive additive are analyzed. Scanning electron microscopy  
 95 (SEM), BET (Brunauer, Emmett and Teller theory) and Ultrapycnometer have been utilized in order to  
 96 determine the shape, specific surface area and density, respectively. Figure 2 shows the SEM images of the

97 filler-sized particles; weak limestone (WL) filler, produced limestone (PL) filler and iron powder (IP). It can  
98 be seen that the angular shape and size of filler limestone – WL and PR – is similar comparing iron powder  
99 (IP) where it presents smaller size and smoother shape than mineral fillers. Moreover, the physical properties  
100 of filler-sized particles of conductive mastics were determined and given in Table 1.

101 In order to investigate the impact of iron powder as filler-sized conductive particle within the asphalt  
102 mastics, two mastic preparation processes are used. The first one is by adding iron powder with replacing an  
103 equivalent volumetric amount of mineral fillers and the other one is without replacing the mineral fillers. It is  
104 important to note that the adding order of filler-sized particles, the mixing time and the mixing temperature  
105 affect on the well-dispersion of asphalt mastics. In the current research, the mixing process is separated in  
106 two stages; (1) adding and mixing filler-sized particles together for 90 sec and (2) adding asphalt binder  
107 which is SBS polymer modified and mixing it together with particles for 120 sec. Mixing is carried out at 180  
108 °C for 180 sec. The compositions of the different conductive asphalt mastics (MA\_F(\_P)) are given in Table  
109 1. The notation MA indicates mastic, F represents filler, P represents iron powder. The values between  
110 brackets indicate the corresponding volume of the components.  
111



112 **FIGURE 2** High magnification SEM SEI images of filler-sized particles; (a) WL, (b) PL and (c) IP  
113

114 **TABLE 1 Physical properties of filler-sized particles and composition of conductive asphalt mastics**  
 115

	Mineral filler (WL)	Mineral filler (PR)	Iron powder (IP)
Specific surface area (m <sup>2</sup> /g)	10.2650	1.9765	1.0066
Density (kg/m <sup>3</sup> )	2780	2698	7507

Type of Asphalt mastic	Density of Asphalt mastic	Mineral filler WL (% m/m)	Mineral filler PR (% m/m)	Iron powder (% m/m)
MA_F100_P0	1.594	50.40	7.10	0.00
MA_F95_P5	1.646	47.88	6.75	7.79
MA_F90_P10	1.683	45.36	6.39	15.58
MA_F85_P15	1.730	42.84	6.04	23.37
MA_F80_P10	1.844	40.32	5.68	31.16
MA_F75_P25	1.957	37.80	5.33	38.95
MA_F50_P50	2.243	25.20	3.55	77.90
MA_F25_P75	2.455	12.60	1.78	116.85
MA_F0_P100	2.796	0.00	0.00	155.80
MA_F100_P25	2.361	50.40	7.10	38.95
MA_F100_P50	3.006	50.40	7.10	77.90

MA: asphalt mastic, F: mineral filler, P: iron powder, bitumen (% m/m): 42.5

116

## 117 **EXPERIMENTAL METHODS**

118

### 119 **SEM Imaging**

120

121 Micrographs of the conductive asphalt mastics are captured using a scanning electron microscope (SEM).  
 122 The micrographs are obtained from a JEOL JSMM 6500F using an electron beam energy of 15 keV and beam  
 123 current of approx. 100 pA. The backscattered electron image mode (BSE) is selected for the images  
 124 acquisition.

125 Aluminum cylinders with a height of 18 mm and a diameter of 31 mm are used as sample-substrates for  
 126 SEM scanning. A thin film of mastic is applied on a glass plate at 140 °C in order to form a very smooth area  
 127 at one side after which the sample is stored at room temperature for 24 hours. Then, the sample is gently cut  
 128 and placed on the aluminum cylinders. The study of micro-morphology of conductive asphalt mastic is  
 129 performed in the environmental mode.

130

### 131 **Electrical and Thermal Properties**

132

133 After mixing the components, the hot conductive asphalt mastic is poured in a silicon-rubber mould to obtain  
 134 rectangular samples with dimension 125 × 20 × 25 mm. Electrical resistivity is determined with the two-  
 135 electrode method at room temperature of 20 °C. The short ends of specimen are cut by 1mm in order to avoid  
 136 the problem of binder concentration at the surface and to have better contact with the electrodes. The  
 137 electrodes are made of copper, placed in the right and left sides of the moulds and with the samples inside the  
 138 mould the electrical volumetric resistance is measured using a digital Multimeter.



139 The geometry and the electrical resistivity of the material are the only parameters that influence the  
 140 resistance. The difference in potential value between the electrodes and their total charge do not play a role  
 141 for this material property. Therefore, the electrical resistivity is obtained from the second Ohm-law:  
 142

$$\rho = \frac{RS}{L} \quad (5)$$

143 where  $\rho$  is the electrical resistivity, measured in  $\Omega\text{mm}$ ,  $L$  is the internal electrode distance, measured in mm,  $S$   
 144 is the electrode conductive area measured in  $\text{mm}^2$  and  $R$  is the measured resistance, in  $\Omega$ .

146 Thermal conductivity measurements are performed by using the C-Therm TCi thermal analyzer. The  
 147 sensor is based on the Modified Transient Plane Source Method to determine the thermal resistivity and  
 148 effusivity of the conductive asphalt mastic. The specimen has a diameter of 17 mm to cover the entire sensor.  
 149 The sensor is heated with a small current and its responses are monitored while in contact with the specimen.  
 150 The thermal resistivity and effusivity of the specimen are measured and obtained directly from the sensor.  
 151 From the inverse of the resistivity the thermal conductivity is obtained. Using the effusivity concept other  
 152 thermal properties such as heat capacity and diffusivity can be derived. The effusivity is given by:  
 153

$$Effusivity = \sqrt{k \cdot \rho \cdot c_p} \quad (7)$$

154 where  $k$  is the thermal conductivity [ $\text{W/m}\cdot\text{K}$ ],  $\rho$  is the density [ $\text{kg/m}^3$ ] and  $c_p$  is the heat capacity [ $\text{J/kg}\cdot\text{K}$ ].  
 155 The thermal conductivity is defined from the Fourier law as:  
 156  
 157

$$q = -k \cdot \frac{dT}{dx} \quad (8)$$

158 where  $q$  is the heat flux (the amount of thermal energy flowing through a unit area per unit time),  $\frac{dT}{dx}$  is the  
 159 temperature gradient and  $k$  is the coefficient of thermal conductivity, often called thermal conductivity. The  
 160 heating, reading and cooling process was repeated 6 times per specimen and the average value was used for  
 161 the analysis.  
 162

### 163 **Frequency Sweep Test**

164 Dynamic Shear Rheometer (DSR) was utilized to obtain the rheological properties of the conductive asphalt  
 165 mastic. Frequency sweep tests are carried out over a temperature range from  $-10\text{ }^\circ\text{C}$  to  $60\text{ }^\circ\text{C}$  and the complex  
 166 modulus and phase angle can be determined. By shifting these mechanical properties to a reference  
 167 temperature (i.e.  $30\text{ }^\circ\text{C}$ ), the master curves of the complex modulus and phase angle are built up for all  
 168 conductive asphalt mastics. Before starting frequency sweep tests, a stress sweep test was conducted in order  
 169 to identify the material linear viscoelastic range (LVR). The LVR is characterized as the 10% stiffness  
 170 reduction criterion and was used to filter the linear and non-linear viscoelastic region.  
 171  
 172

### 173 **Multiple-Stress Creep Recovery Test**

174 Apart from the frequency sweep analysis, DSR is also used to conduct the Multiple Stress Creep Recovery  
 175 Test (MSCRT) at high service temperature. This test has been developed by FWHA as result of refinements  
 176  
 177

178 in the repeated creep and recovery test and it basically consists of applying subsequent loading-unloading  
179 cycles monitoring the accumulated strain levels at each cycle (20). The presence of the elastic response of the  
180 asphalt mixtures is defined by determining the percentage recovery and non-recoverable compliance.  
181 Notably, the non-recoverable creep compliance denotes the rutting resistance or the permanent deformation  
182 sensitiveness of asphalt mixture under repeated loading and that can be determined using the MSCR test (21,  
183 22).

184 According to AASHTO TP 70-10 standard, the conductive asphalt mastics are loaded at a constant stress  
185 for 1 s and then allowed to recover for 9 s. Ten creep and recovery cycles are run at 0.1 kPa creep stress  
186 followed by ten more cycles at 3.2 kPa creep stress. The stress and strain are recorded at least every 0.1  
187 seconds for the creep cycle and at least every 0.45 seconds for the recovery cycle during the test. The percent  
188 recoveries and the non-recoverable compliance were obtained at the end of each cycle and the average values  
189 were used at each loading level.

190 Here, multiple stress creep and recovery tests were carried out at 64 °C and the tests were performed with  
191 the parallel plate geometry with diameter 25 mm and 1 mm gap. The asphalt mastic samples were allowed to  
192 reach constant temperature for 10 minutes (within +/- 0.1 °C tolerance). Two replicates of each mastic were  
193 used for analysis and the rutting potential of each was evaluated at high temperatures. It should be noticed  
194 that the test described above is normally done on pure binders, so the results are only for comparison the  
195 different mastics under the given loading conditions.

196

## 197 **RESULTS**

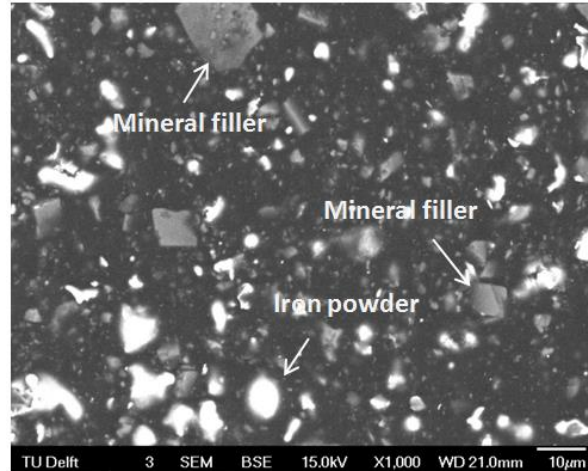
198

### 199 **Micro-Morphological Images**

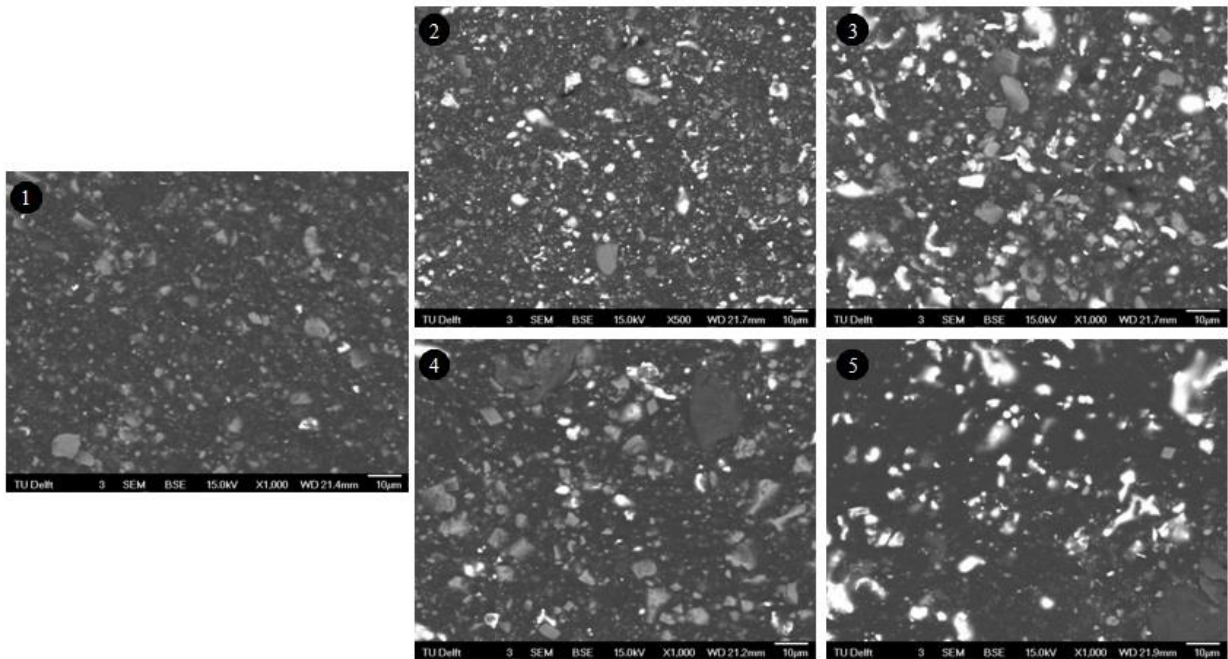
200

201 The surface micro-morphology of asphalt mastic with iron powder is presented in Figure 3.a. The different  
202 conductive asphalt mastics with different amounts of iron powder as described in Table 1 are investigated.  
203 The grey particles represent the mineral fillers and the brightest parts of the images are the iron powder. By  
204 comparing images 3 and 5 in Figure 3.b, it is obvious that the conductive asphalt mastics without substituting  
205 the mineral filler - see image 3 - appear to have a surface morphology with less dark space than asphalt  
206 mastics produced with substituting mineral filler with iron powder, see image 5. The spacing among the  
207 filler-sized particles is reducing with increasing the amount of iron powder without substituting relative  
208 volumetric amount of mineral filler, see images 1 to 3. Qualitative observation of conductive asphalt mastics  
209 surfaces with SEM shows that the morphology of asphalt mastics after adding iron powder has a direct link  
210 with the volumetric concentration of filler-sized particles – iron powder and mineral fillers. It should be noted  
211 that the current micro-morphological results agree with the rheological results of conductive asphalt mastics  
212 which will be explained in the Frequency Sweep Test subsection of the current paper.

213



(a)



(b)

214 **FIGURE 3 SEM BSE (a) image of a conductive asphalt mastics with iron powder and (b) images of**  
 215 **conductive asphalt mastics demonstrating the influence of replacing mineral filler with iron powder on**  
 216 **the micro-morphology: (1) MA\_F100\_P0, (2) MA\_F100\_P25, (3) MA\_F100\_P50, (4) MA\_F75\_P25 and**  
 217 **(5) MA\_F50\_P50**

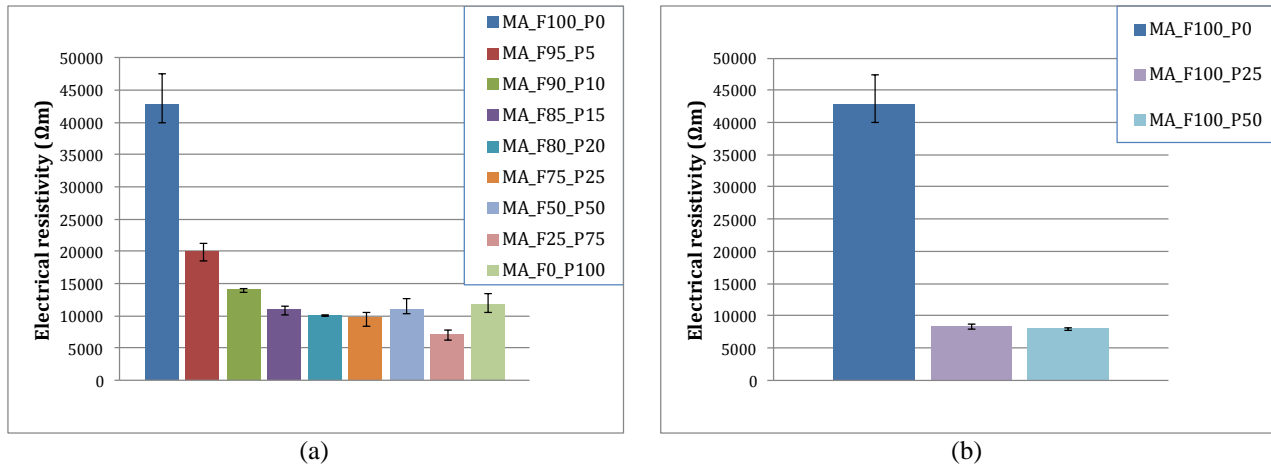
218

### 219 **Electrical and Thermal Properties**

220

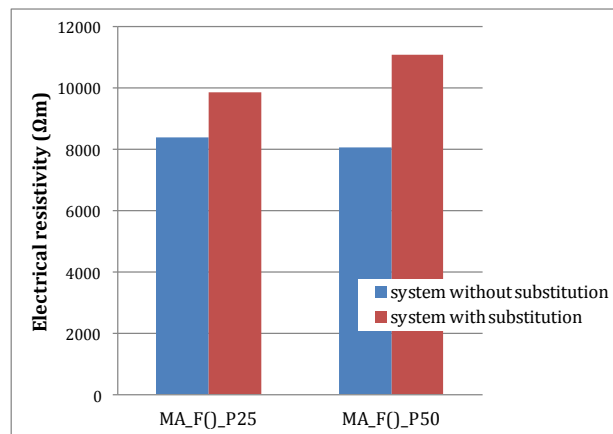
221 The electrical resistivity decreases with increasing iron powder content with or without replacing an  
 222 equivalent proportion of mineral filler, see Figure 4. In Figure 4.a, a reduction of the electrical resistivity is  
 223 observed when iron powder is mixed proportionally within the asphalt mastic by substituting mineral filler.

224 Moreover, Figure 4.b shows that the resistivity was also reduced after adding extra iron powder into the  
 225 asphalt mastic matrix. The reason of this decrease of the electrical resistivity can be explained by the  
 226 percolation threshold theory. The percolation threshold was reached when the shorter conductive pathways  
 227 were formed by the higher amount of iron powder in the asphalt mastic. The conductive asphalt mastic  
 228 MA\_F85\_P15 represents the mastic at the percolation threshold position and adding more iron powder hardly  
 229 reduces the electric resistivity further.  
 230



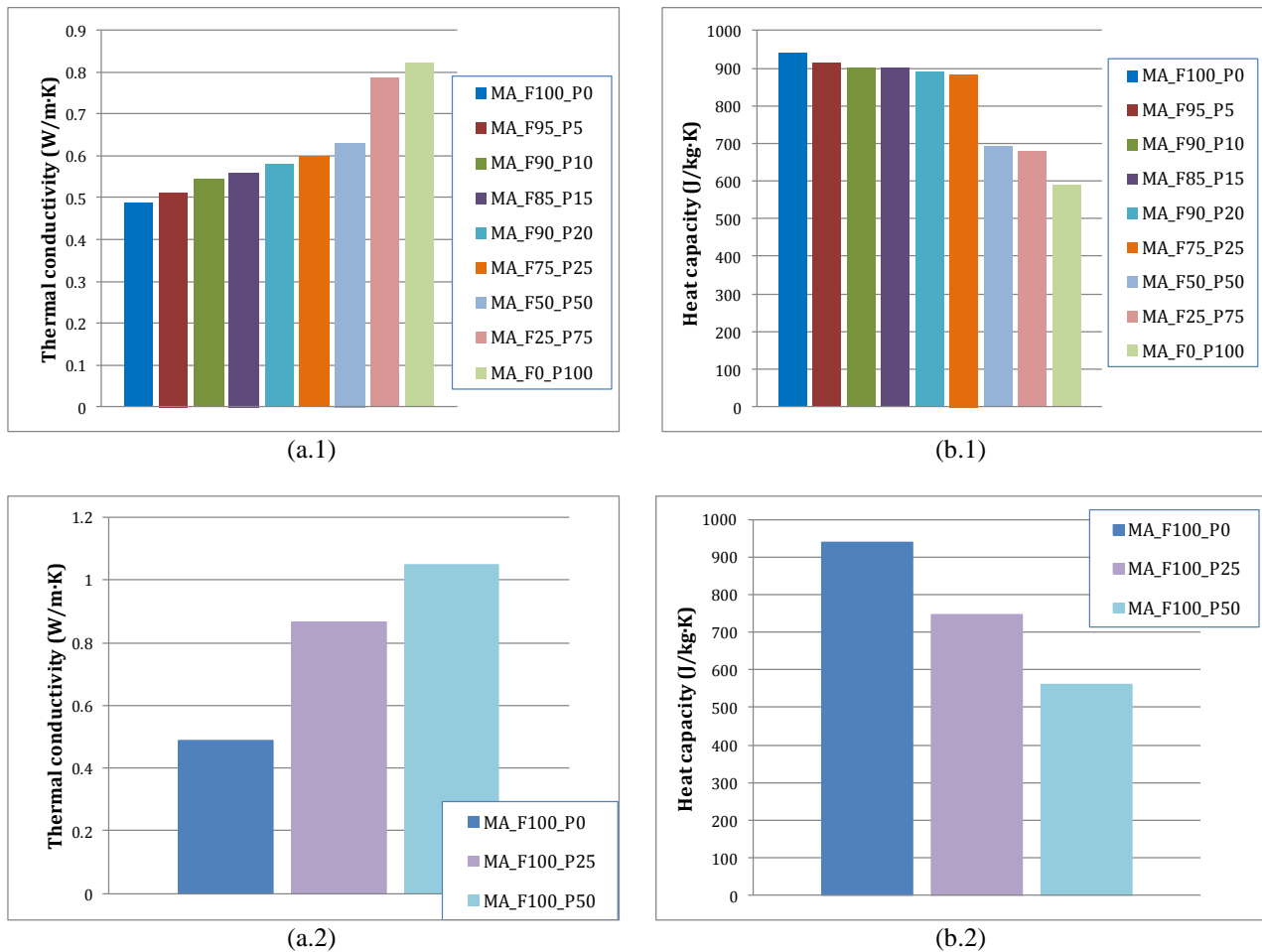
231 **FIGURE 4 Effect of the volume content of iron powder on (a) the electrical resistivity of conductive**  
 232 **asphalt mastics after replacing mineral filler with iron powder and (b) the electrical resistivity of**  
 233 **conductive asphalt mastics without replacing mineral filler with iron powder**  
 234

235 Finally, the conductive asphalt mastics without replacing of mineral fillers with iron powder show a lower  
 236 electrical resistivity than those developed after replacement, see Figure 5. This observation happens because  
 237 the filler-sized particles form a highly density skeleton with very short spacing between the particles when  
 238 extra iron powder is added in the asphalt mastic.  
 239



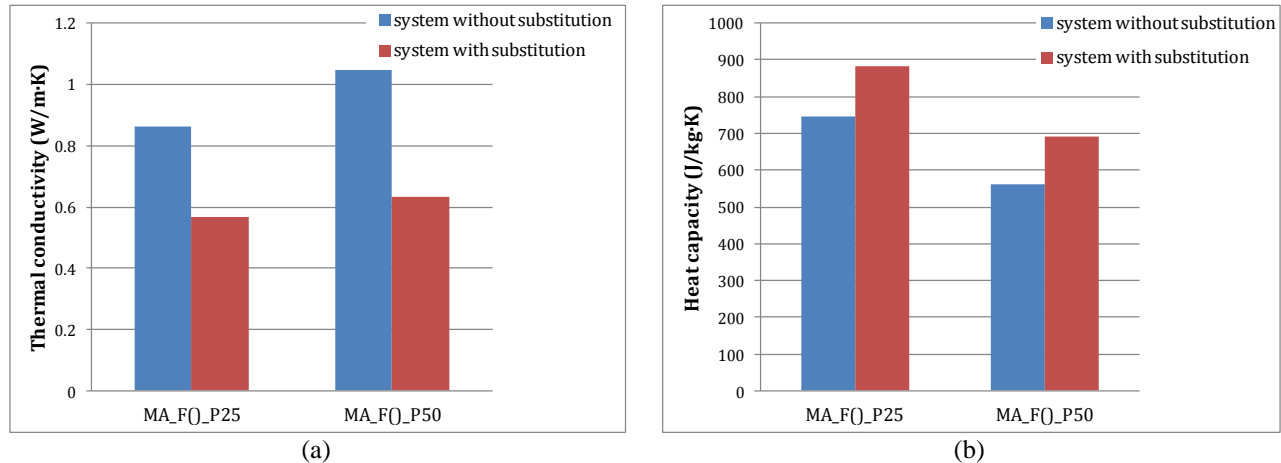
240 **FIGURE 5 Effect of developing conductive asphalt mastics with and without replacing part of mineral**  
 241 **filler with iron powder on electrical conductivity**  
 242  
 243  
 244

245 The thermal conductivity and heat capacity of asphalt mastics produced, with and without substituting part  
 246 of the mineral filler with iron powder, are presented in Figure 6. It was found that the thermal conductivity of  
 247 asphalt mastic increased after adding iron powder. This increasing tendency can be explained by the thermal  
 248 properties of iron powder which is added into the asphalt mastic. It is known that the thermal conductivity of  
 249 iron powder is considerably higher than the conductivity of the other asphalt components. Hence the increase  
 250 of the amount of iron powder leads to an increase of the effective thermal conductivity of the conductive  
 251 asphalt mastic. This can be seen in Figure 6.a1&a2 showing that the thermal conductivity of sample  
 252 MA\_F85\_P15, which represents the conductive asphalt mastic at the electrical percolation threshold, was  
 253 0.56 W/mK is higher than the thermal conductivity of pure asphalt mastic sample MA\_F100\_P0 which was  
 254 0.487 W/mK. On the other hand, Figure 6.b1&b2 demonstrates a reduction of the heat capacity of asphalt  
 255 mastics when iron powder is added.  
 256



257 **FIGURE 6** Effect of the volume content of filler-size additives on (a.1) the thermal conductivity and  
 258 (b.1) heat capacity of conductive asphalt mastics after substituting mineral filler with iron powder,  
 259 (a.2) the thermal conductivity and (b.2) heat capacity of conductive asphalt mastics without  
 260 substituting mineral filler with iron powder  
 261

262 Finally, the produced conductive asphalt mastics without substitution of mineral filler-sized particles had a  
 263 higher thermal conductivity and lower heat capacity, see Figure 7. At higher filler-sized particles  
 264 concentration, the interaction among the particles is increasing within the asphalt mastics. Thus, the spacing  
 265 among the particles and the coating role of asphalt binder around the particles reduces having as consequence  
 266 this thermal observation for the conductive asphalt mastics.  
 267



268 **FIGURE 7 Effect of developing conductive asphalt mastics with and without substitution of mineral**  
 269 **filler with iron powder on (a) thermal conductivity and (b) heat capacity**

270

### 271 Frequency Sweep Test

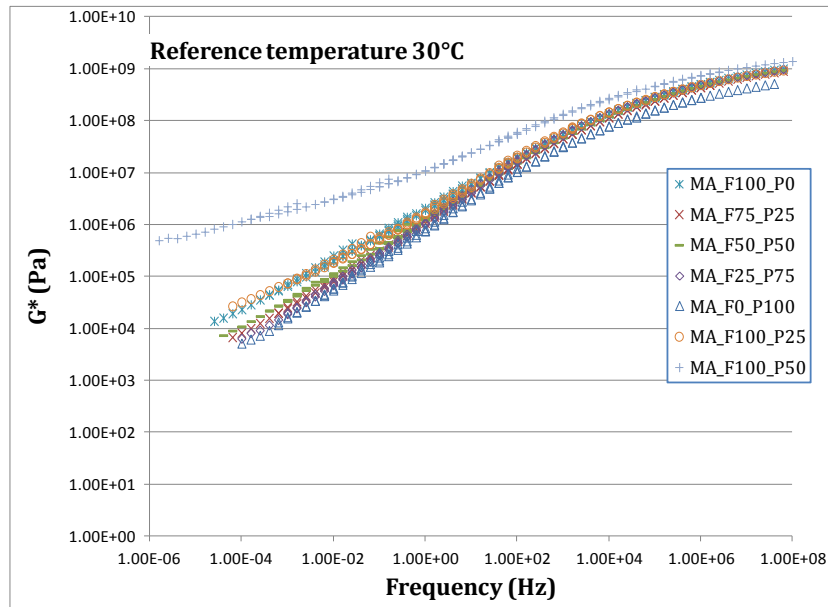
272

273 Before the frequency sweep tests, the stress sweep test was conducted from  $-10\text{ }^{\circ}\text{C}$  to  $60\text{ }^{\circ}\text{C}$  with a shear stress  
 274 range from 0.01 to 10 Pa and at 1 Hz in order to identify the linear viscoelastic range (LVR). The LVR is  
 275 characterized as the 10% stiffness reduction criterion and was used to filter the linear and non-linear  
 276 viscoelastic region. Afterwards, the frequency sweep test was carried out over a temperature range from  $-10$   
 277  $^{\circ}\text{C}$  to  $60\text{ }^{\circ}\text{C}$ . At a reference temperature of  $30\text{ }^{\circ}\text{C}$ , the master curves as given in Figure 8 show the rheological  
 278 behavior for all the conductive asphalt mastics. The test stress sweep and frequency sweep were run on 8 mm  
 279 parallel plates with a 2 mm gap for mastics at all the testing temperatures.

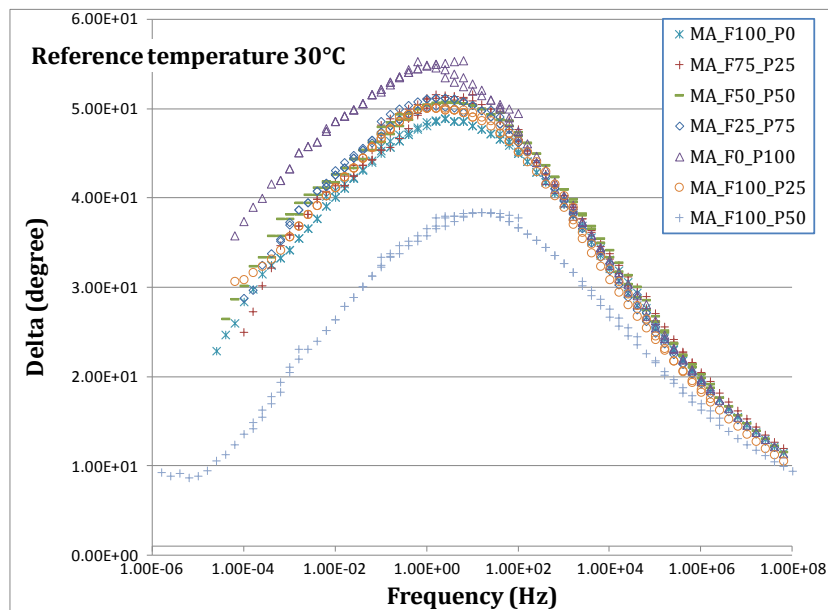
280 It can be observed that the asphalt mastic without adding iron powder is obviously much stiffer than the  
 281 conductive mastics produced after replacing mineral filler with iron powder. This happens due to the fact that  
 282 iron powder is spherical and finer particle than the other mineral fillers and is easily rolling under shear stress  
 283 when is added in the mastic by replacing mineral filler. However, the asphalt mastics appear to have a higher  
 284 complex modulus and lower phase angle when iron powder is added without replacing the mineral filler. The  
 285 reducing visco-elastic properties at higher concentrations of filler-sized particles and when particles are added  
 286 without substitution are linked with the interaction of particle-particle. Increasing the concentration of filler-  
 287 sized particles leads to lower the spacing among the particles and asphalt mastics with lower viscosity and  
 288 higher stiffness are obtained. Consequently, the lower workability of mastic during mixing process is  
 289 resulted.

290

291



(a)



(b)

292 **FIGURE 8 (a) Complex modulus and (b) phase angle master-curves for conductive asphalt mastic**  
 293 **produced with and without substitution part of filler with iron powder**

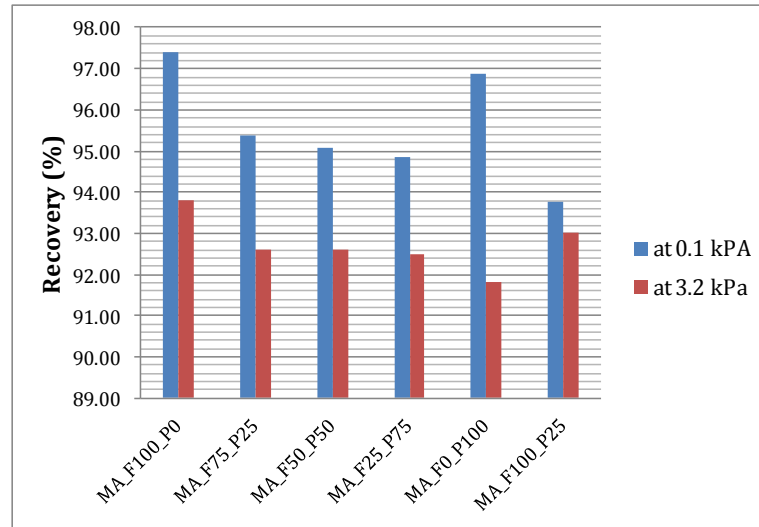
294

295 **Multiple-Stress Creep Recovery Test**

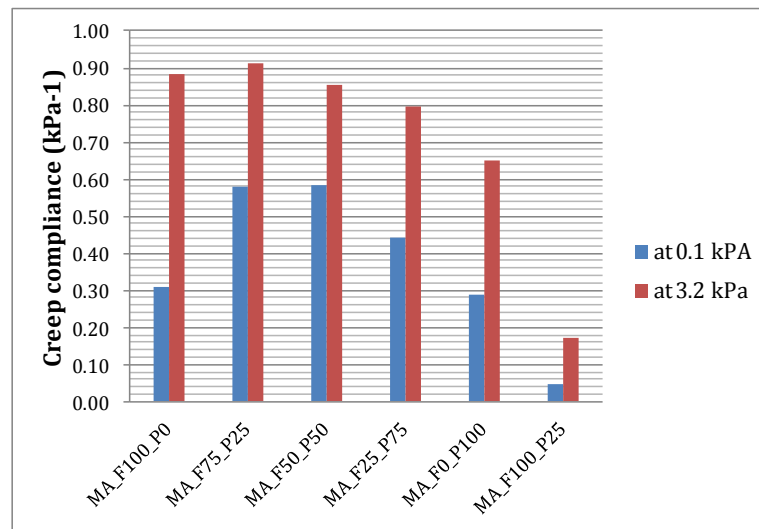
296

297 MSCR test was used to quantify the rutting sensitivity of conductive asphalt mastics and for this reason the  
 298 percent recovery and the non-recoverable compliance were determined at two different stress levels. Figure  
 299 9.a shows that the percent recovery of the conductive asphalt mastics experienced a slight reduction from

300 97.5% to 95% for MA\_F100\_P0 and MA\_F0\_P100 respectively, at lower stress level. This slight reduction  
 301 indicates that the conductive asphalt mastics can recover a lower portion of the total strain at the end of each  
 302 loading-unloading cycle for the lower load level. Similarly, reduction of the percentage recovery shows the  
 303 same tendency for the higher stress level for the same mastics. This observation of lower percent recoveries  
 304 indicate that conductive mastics appear marginally higher prone to rutting when iron powder substitutes  
 305 mineral filler. Moreover, conductive mastics demonstrate reduction of the percent recovery as well when iron  
 306 powder was added without replacing part of mineral filler.  
 307



(a)



(b)

308 **FIGURE 9 (a) Recovery (%) and (b) non-recoverable creep compliance (kPa<sup>-1</sup>) of conductive asphalt**  
 309 **mastics**

310  
 311 The non-recoverable compliances of conductive asphalt mastics are illustrated in Figure 9.b. High  
 312 compliance values of mastic imply that the rutting performance is weak. It can be observed that significant



313 decrease of the creep compliance is found in case of producing conductive asphalt mastics by adding iron  
314 powder (MA\_F100\_P25). This means that mastic MA\_F100\_P25 can accumulate plastic deformations by  
315 heavy traffic loads sufficiently. However, as noticed in Frequency Sweep results subsection, the visco-elastic  
316 properties of mastics produced with adding iron powder, such as MA\_F100\_P25, were reduced (lower  
317 viscosity and higher stiffness) and subsequently the workability of asphalt mixture lowers. About the mastics  
318 produced by replacing mineral filler with iron powder, these appear a minor increase at 0.1 kPa stress level  
319 when 25% of iron powder was added. The creep compliance shows similar performance for both low and  
320 high stress level such as the percent recovery response of mastics.

321

## 322 CONCLUSIONS

323

324 As it is mentioned several times on this paper, the type of filler-sized particles, the concentration of particles  
325 and the interaction among particles and asphalt binder have direct influence on structural and non-structural  
326 performance of asphalt mastics. Here an experimental protocol was proposed with main objective to explore  
327 the impact of filler-sized particles on the performance asphalt mastics produced for induction heating  
328 applications.

329 For these purposes, as well as for the purpose of improving the electrical and thermal properties of asphalt  
330 mastics, iron powder was selected as filler-sized additive. During this research, it became clear that  
331 understanding the conductive additives-mineral fillers interaction within the binder matrix provides the  
332 necessary framework not only to control the electro-thermal properties but also to adjust the workability of  
333 mastic at desired levels. Viscosity, effective electrical and thermal conductivity of mastics were assessed as  
334 the most valuable parameters to manufacturing more durable asphalt mixtures with induction heating  
335 capabilities.

336 Future studies should include more fundamental parameters of filler-sized particles of mastics, such as  
337 chemical and electrochemical studies on the particles-particles and the particles-binder interactions.  
338 Moreover, the evaluation of moisture and chloride induced damage of conductive asphalt mastics and  
339 subsequently of asphalt concrete mixtures has been assessment crucial to predict the proper time of induction  
340 heating maintenance of asphalt pavement.

341

## 342 ACKNOWLEDGEMENTS

343

344 The authors would like to thank Heijmans-Breijn for its financial support on this project. Gratitude is also  
345 expressed to K. Kwakernaak and N. Zhong of Delft University of Technology for the SEM and C-Therm TCi  
346 thermal testing.

347

## 348 REFERENCES

349

- 350 1. European Asphalt Pavement Association. *The Asphalt Paving Industry: a global perspective*. Brussels.  
351 2011.
- 352 2. Transportation Research Center. *Managing Urban Traffic Congestion- Summary Document*. Joint  
353 Transportation Research Center, 2004.
- 354 3. Thodesen, C., A. Carrera, A. Dawson. *Future Rehabilitation and Maintenance & Cost-Benefit Study of*  
355 *Alternative Solutions: Report N. 10*, Road Research in Europe – road ERA.net, 2010.
- 356 4. Garcia, A., E. Schlangen, M. van de Ven, Q. Liu. Electrical Conductivity of Asphalt Mortar Containing  
357 Conductive Fibers and Fillers. *Construction and Building Materials*, Vol. 23, 2009, pp. 3175-3181.

- 358 5. Liu, Q., E. Schlangen, M. van de Ven, A. Garcia. Induction Heating of Electrically Conductive Porous  
359 Asphalt Concrete. *Construction and Building Materials*, Vol. 24, 2010, pp. 1207-1213.
- 360 6. Liu, Q., A. Garcia, E. Schlangen, M. van de Ven. Induction Healing of Asphalt Mastic and Porous  
361 Asphalt Concrete. *Construction and Building Materials*, Vol. 25, 2011, pp. 3746-3752.
- 362 7. Liu, Q., E. Schlangen, M. van de Ven, G. van Bochove, J. van Montfort. Evaluation of the Induction  
363 Healing Effect of Porous Asphalt Concrete through Four Point Bending Fatigue Test. *Construction and  
364 Building Materials*, Vol. 29, 2010, pp. 40-409.
- 365 8. Garcia, A., J. Norambuena-Contreras, M.N. Partl. Experimental Evaluation of Dense Asphalt Concrete  
366 Properties for Induction Heating Purposes. *Construction and Building Materials*. Vol. 46. 2013, pp. 48-  
367 54.
- 368 9. Garcia, A., J. Norambuena-Contreras, M.N. Partl, P. Schuetz. Uniformity and Mechanical Properties of  
369 Dense Asphalt Concrete with Steel Wool Fibers. *Construction and Building Materials*, Vol. 43, 2013, pp.  
370 107-117.
- 371 10. Garcia, A., J. Norambuena-Contreras, M.N. Partl. A Parametric Study on the Influence of Steel Wool  
372 Fibers in Dense Asphalt Concrete. *Materials and Structures*, Vol. 47, 2014, pp. 1559-1571.
- 373 11. Anderson, D.A., W.H. Goetz. Mechanical Behavior and Reinforcement of Mineral Filler-Asphalt  
374 Mixtures. *Asphalt Paving Technology*. AAPT, Vol. 42, 1973, pp.37-66.
- 375 12. Anderson, D.A., H.U. Bahia, R. Dongre. Rheological Properties of Mineral Filler-Asphalt Mastics and its  
376 Importance to Pavement Performance. In: *Richard C. Meininger, ed. Effects of Aggregates and Mineral  
377 Fillers on Asphalt Mixture Performance: ASTM STP 1147*. 1992.
- 378 13. Smith, B.L. S.A.M. Hesp. Crack Pinning in Asphalt Mastic and Concrete: Regular Fatigue Studies.  
379 *Transportation Research Record*, 1728, 2000, pp. 75-81.
- 380 14. Castelo Branco, V.T.F. Fatigue Analysis of Asphalt Mixtures Independent of Mode of Loading.  
381 *Transportation Research Record*, 2057, 2008, pp. 149-156.
- 382 15. Valenta, R., M. Sejnoha, J. Zeman. Macroscopic Constitutive Law for Mastic Asphalt Mixtures from  
383 Multiscale Modelling. *Journal for Multiscale Computational Engineering*, 8 (1), 2010, pp. 131-149.
- 384 16. Collop, L. A., M. Stroup-Gardiner, E.R. Brown, D.I. Hanson, M.O. Fletcher. Characterisation of Asphalt-  
385 Filler Mortars with Superpave Bitumen Tests. *Association of Asphalt Paving Technologists*, 1998.
- 386 17. Wu, S., P. Pan, F. Xiao. Conductive Asphalt Concrete: A Review on Structure Design, Performance and  
387 Practical Applications. *Journal of Intelligent Material Systems and Structures*, 2013.
- 388 18. Wu, S., L. Mo, Z. Shui, Z. Chen. Investigation of the Conductivity of Asphalt Concrete Containing  
389 Conductive Fillers. *Carbon*, 43, 2005, pp. 1358-1363.
- 390 19. Park, P. Y. Rew, A. Baranikumar. *Controlling Conductivity of Asphalt Concrete with Graphite*. Texas  
391 A&M Transportation Institute College Station, Report No SWUTC/14/600451-00025-1. 2014.
- 392 20. Domingos, M.D.I., A.L. Faxina. Creep-Recovery Behavior of Modified Asphalt Binders with Similar  
393 High-Temperature Performance Grades. *TRB 2014 Annual Meeting*, 2014.
- 394 21. D'Angelo, J., R. Kluttz, R.N. Dongre, Stephens K., Zanzotto L. Revision of the Superpave High  
395 Temperature Binder Specification: The Multiple Stress Creep Recovery Test. *Journal of the Association  
396 of Asphalt Paving Technologists*, 76, 2007.
- 397 22. D'Angelo, J., R. Dongre. Practical Use of Multiple Stress Creep and Recovery Test. *Transportation  
398 Research Record: Journal of the Transportation Research Board*, No. 2126, 2009. Transportation  
399 Research Board of the National Academies. Washington, DC. 2009. pp. 73-82.